

UDC 622.2:614.83 (075.8)

V. N. TYUPIN¹, Professor, Doctor of Engineering Sciences, tyupinvn@mail.ru**E. B. YANITSKY**², Deputy Chief Executive Officer, Candidate of Geographic Sciences**A. E. POLYAKH**³, Technical Officer**I. M. IGNATENKO**¹, Head of Institute, Candidate of Engineering Sciences¹Belgorod State National Research University, Belgorod, Russia²JSC VIOGEM, Belgorod, Russia³LLC Special Operations, Murmansk, Russia

SEISMICALLY SAFE PARAMETERS OF CONFINED BLASTING IN LEVELLING DRY DOCK BOTTOM

Introduction

The dry dock construction works in the Murmansk Region faced an unforeseen task of blasting to be carried out between a caisson and a cofferdam between the dry dock and the gulf (Fig. 1). The goal was to level hard rock surface down to 16.2 m. Blasting was to be performed so that to maintain integrity of caisson 2 and soil–cement piles 3 in cofferdam 4 to avoid flooding of the dry dock under construction. Moreover, it was required to ensure the assigned fragmentation quality of rocks as the rock mass blocks were 0.5–1.0 m in size while the loading equipment had the bucket capacity of 1.0 m³, which meant that the permissible fragment size was 0.75 m. Fragmentation of oversizes by additional blasting or using machines can infract the construction technologies and impair the safety.

The blasting site at the land wall of the dry dock is composed of gneiss and gneissic granite and exceeds the required grade elevation of 16.2 m by 7.0 m nearby the caisson with a depression to 0.7 m gulfward (see fig. 1). On the whole, the higher elevation site is 53 m wide and around 220 m long. The blasting site is 10–12 m wide and 220 m long.

The granite and gneissic granite rock mass has the bulk weight of $(2.66–2.77) \times 10^3$ kg/m³, the elasticity modulus of $(1.2–2.1) \times 10^{10}$ Pa, Poisson's ratio of 0.3, the ultimate compression strength of 76–118 MPa, the ultimate tension strength of 3.5 MPa and the hardness factor of 10. A block size in the granite and gneissic granite rock mass is 0.5–1.0 m upon average and sometimes reaches 2.0 m. The rock mass is wet.

The hard rock mass in the cofferdam is overlaid with a layer of platy sand clay with pebbles (40%) and boulders (EGE 422 and 222). The wet soil has the bulk weight 2200–2270 kg/m³ and the porosity factor of 0.440–0.337. The upper-lying layer composed of fine sand and pebble (to 45%) with average density boulders is also wet (EGE 214) and has the porosity factor of 0.681.

The soil–cement piles meant to ensure impermeability of the cofferdam have the density of 2000 kg/m³, P-wave velocity of 2100 m/s, Poisson's ratio of 0.4, as well as the ultimate compression and tension strengths of 1.5 MPa and 0.1 MPa, respectively. The reinforced concrete caisson has the density of 2350 kg/m³, P-wave velocity of 4700 m/s and Poisson's ratio of 0.2.

This study aims at the drilling-and-blasting pattern design and substantiation to ensure integrity of the caisson and soil–cement piles in the cofferdam, levelling the hard rock mass site down to 16.2 m and the quality rock fragmentation.

During construction of a dry dock, it became necessary to level the bottom of gneissic granite rock mass to 7 m by blasting. The blasting site appeared to be spaced at 8.5–20.0 m from a reinforced concrete caisson and a sand cofferdam reinforced with soil–cement piles. Aiming to ensure the required levelling at 16.2 m, the preset fragmentation quality and the reduced seismic safety, the parameters associate with the drilling-and-blasting pattern were calculated. The values of PPV caused by blasting-induced seismic waves in the caisson and cofferdam were found from the constructed formulas. The experimental measurement of ground vibrations induced by blasting used seismic recorder Vibracord DX. Al in all, 20 large-scale blasts were performed, and the blasted rock volume totaled 9 Km³.

The comparison of the actual and calculated values of PPV in the caisson and cofferdam proves reliability of the presented formulas. It is calculated that PPV caused by the blasting-induced seismic waves at the farther wall of the caisson and at the nearest wall of the soil–cement piles are 2.0–27.0 mm/s and 2.0–22.0 mm/s, respectively, which is much less than the allowable PPV of 100–500 mm/s for the hydraulic engineering structures. It has been determined during blasting that the caisson preserves its integrity and no increase in the water inflow from the gulf is observed.

Keywords: blasting, confined conditions, blasting-induced seismic effect, caisson, cofferdam, soil–cement piles, physicochemical properties, calculation formulas, PPV, seismograms, reliability

DOI: 10.17580/em.2022.02.04

Methodology

Acquisition and analysis of information on the physicochemical properties of the gneissic granite rock mass, caisson and cofferdam. Justification of the formulas to calculate blasting-induced seismic waves (BSW) at the caisson and cofferdam. Numerical calculation of PPV caused by BSW in different directions. Experimental measurement of ground vibrations using Vibracord DX recorder. Analysis and comparison of theoretical and experimental results. Validation of the proposed formulas.

Justification of drilling-and-blasting pattern design to ensure seismic safety and quality fragmentation

To minimize the seismic impact of blasting in levelling the base and horizontal location of the dry dock, the vertical blastholes has a diameter of 64 mm. The softening blasthole charge is a continuous column. A charging cartridge of Nitronit-P is placed at the bottomhole, at the level of the sole of the blasting layer. The main explosive charges are cartridges of Nitronit-P with a diameter of 45 mm. The blasting network uses electronic initiation system Orika i-con. The short-delay blasting pattern can have the shape of a wedge or a trapezoid, and includes short delays between charges. The delay interval is chosen to be 50 ms to prevent interference of blasting-induced seismic waves generated by successively detonated charges.

The blasting pattern design to reach the preset fragmentation quality is determined using the studies [1, 2]: the blasthole pattern is 1.6×1.6 m; the burden line is 1 m; the overdrill is 1.0 m; the explosive charge is 5.4–8.2 kg per blasthole; the powder factor is 0.5–0.8 kg/

m³. To minimize the seismic impact of blasting on the caisson and cofferdam, the blasting block is 5 m wide and 10–20 m long, and has 20–40 blastholes.

Blasting was performed by Special Operations LLC. Protection from fragment dispersion and air blast is effectively ensured via placement of multi-layered metal sheets on the blasting site. All in all, 20 blocks were blasted. The blasted rock volume totaled 9000 m³.

Seismically safe parameters of blasting at caisson and cofferdam

The caisson and cofferdam are the hydraulic engineering structures. According to point 795 [3], regarding bridges, reactors, hydraulic engineering structures and radio towers, seismic safety is an issue to be addressed by special (science and expertise) agencies; in our case, it was VIOGEM JSC. As per [4], the allowable value of PPV induced by BSW is 100–500 mm/s.

Seismic safety in confined blasting is a subject of research both in Russian [5–16] and abroad [17–21]. These works present the experimental, analytical and theoretical studies, discussions and proofs of reliability or appropriateness of the results. The promising and advanced methods use the computer technologies of 3D block modeling [22–25].

The levelling-purpose blasting in the dry dock features adjacency to the caisson and cofferdam which are 8.5–20 m away of the blasting site (see fig. 1). Seismic safety of these objects needs calculating PPV generated by BSW in three directions, namely: direction 12 (see fig. 1) toward the nearest wall of the caisson, direction 13 under the caisson bottom, and direction 11 toward the cofferdam with reinforcement represented by two rows of soil–cement piles.

In direction 12 the blasting-induced seismic waves pass the gneissic granite rock mass, the layer of blasted rocks, sand and pebble (EGE 214) and, then, the manmade layer of bagged expanded-clay aggregate.

PPV of ground vibrations due to BSW toward the nearest wall of the caisson (direction 12) is calculated from the formula [14, 16]:

$$u_1(R) = \frac{\sqrt{\pi} D \rho_{ch} d_{ch} c}{8 R \rho_{go} c_{go}} \left(1 - \frac{\mu \nu}{1 - \nu} \right) \left(\frac{\Delta_1}{\Phi_1} + \frac{\Delta_2}{\Phi_2} + \frac{\Delta_3}{\Phi_3} \right) K_{1-4}, \quad (1)$$

where D is the detonation velocity; ρ_{ch} is the charging density; d_{ch} is the explosive charge diameter; c is the P-wave velocity in rock mass in the blasting area; c_{go} is the P-wave velocity in the guarded object; μ is the rock friction coefficient in the blasting area; ν is Poisson's ratio of rocks in the blasting area; $K_{1-4} = K_1 K_2 K_3 K_4$, K_1 is the factor of blasting effect enhancement in perpendicular to the group of charges subjected to simultaneous explosion; K_2 is the factor of blasting effect enhancement in perpendicular to the planes of the blasthole rows beyond the blasting perimeter in short-delay blasting; K_3 is the factor of blasting effect enhancement as function of the blasthole length; K_4 is the response factor which means the energy transferred to the adjacent rock mass in the blasting area; R is the distance from the blast to the guarded object; ρ is the bulk weight of rock mass in the blasting areas; $\pi = 3.14$; Φ_1 is the gneissic granite jointing index; Φ_2 is the sand deformability index (EGE 214); Φ_3 is the expanded-clay aggregate deformability index;

$$\Delta_1 = r_1/R, \Delta_2 = r_2/R, \Delta_3 = r_3/R, \quad (2)$$

where r_1, r_2, r_3 are the thicknesses of the layers of rocks, sand EGE 214 and expanded-clay aggregate, respectively.

In direction 13, BSW propagate in the gneissic granite rock mass and refract under the caisson bottom. The impact pattern is depicted in fig. 1 and the formula is given by:

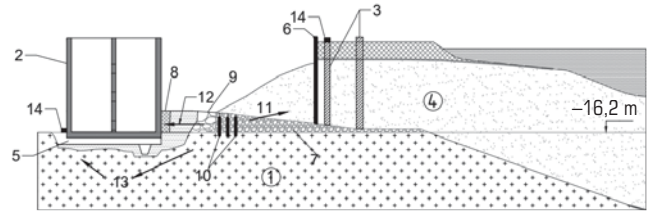


Fig. 1. Layout of gneissic granite rock mass (1), caisson (2), soil–cement piles (3) and blasting site; 4 – sand and sand clay; 5 – caisson foundation bed; 6 – metallic retention wall; 7 – gneissic granite rock mass to be treated; 8 – cushioning bags filled with expanded-clay aggregate; 9 – blasted rocks; 10 – blastholes; 11, 12 and 13 – directions of blasting-induced seismic waves; 14 – locations of geophones

$$u_2(R) = \frac{\sqrt{\pi} D \rho_{ch} d_{ch} c}{8 R \Phi_1 \rho_{go} c_{go}} \left(\frac{\nu}{1 - \nu} \right) \left(1 - \frac{\mu \nu}{1 - \nu} \right) K_{1-4}. \quad (3)$$

In direction 11 BSW pass the gneissic granite rock mass and the layer of fine sand and pebble (EGE 214), and affect the soil–cement pile reinforcement in the cofferdam; the formula is given by:

$$u_3(R) = \frac{\sqrt{\pi} D \rho_{ch} d_{ch} c}{8 R \rho_{go1} c_{go1}} \left(1 - \frac{\mu \nu}{1 - \nu} \right) \left(\frac{\nu_1}{1 - \nu_1} \right) \left(\frac{\Delta_{11}}{\Phi_1} + \frac{\Delta_{12}}{\Phi_2} \right) K_{1-4}, \quad (4)$$

where ρ_{go1} and c_{go1} , respectively, are the density and P-wave velocity in the soil–cement piles; ν_1 is Poisson's ratio of the piles; Δ_{11} is the relative thickness of the rock layer; Δ_{12} is the relative thickness of the sand EGE 214 layer.

Numerical analysis

The calculations of PPV in directions 11–13 from formulas (1)–(4) assume the following values of the involved parameters: explosive is Nitronit-P, blasting is carried out by single blastholes at the delay intervals of 50 ms, the charge length is 4.1 m; $D = 3 \times 10^3$ m/s; $\rho_{ch} = 600$ kg/m³; $d_3 = 0.064$ m; $c = 2.7 \times 10^3$ m/s; $\mu = 0.4$; $\nu = 0.3$; $\rho_{go} = 2.35 \times 10^3$ kg/m³; $c_{go} = 4.7 \times 10^3$ m/s; $R = 8.5$ m; $\Delta_1 = 0.18$; $\Delta_2 = 0.7$; $\Delta_3 = 0.12$; $\Phi_1 = 5.7$; $\Phi_2 = 750$; $\Phi_3 = 462$; $K_1 = 1$; $K_2 = 1$; $K_3 = 1.63$; $K_4 = 0.8$ [14–16]; $K_{1-4} = 1.3$.

Placement of the numerical values in (1)—direction 12—yields the maximum value of PPV $u_1(R) = 0.0257$ m/s or 25.7 mm/s. The permissible value of PPV for the hydraulic engineering structure is 100–500 mm/s. Accordingly, the caisson wall nearest to the blasting site is damage-free.

Insertion of the numerical values in (3) – direction 13 – offers an analytical relation between PPV at the caisson bottom and the distance: $u_2(R) = 0.504R^{-1}$.

Such relation and in such form is necessary as geophones are placed at different distances from the blasting site.

Substitution of the above-listed numerical values, as well as $\rho_{ch1} = 2 \times 10^3$ kg/m³; $c_{ch1} = 2.1 \times 10^3$ m/s; $\nu_1 = 0.4$; $\Delta_{11} = 0.1$; $\Delta_{12} = 0.9$ in (4)—direction 11—produces the dependence of PPV in the soil–cement piles on the distance: $u_3(R) = 0.22R^{-1}$.

Experiment, results and discussion

The ground vibration measurements used seismic recorder Vibracord DX. During blasting, from 3 to 5 geophones are placed at the farther wall

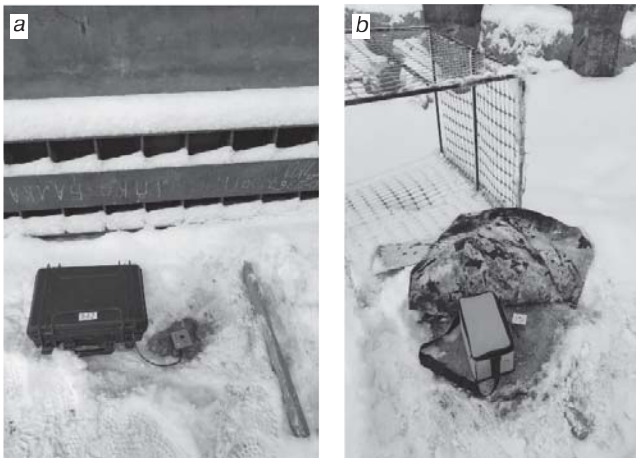


Fig. 2. a – Geophone arranged on caisson foundation bed (large-scale blast no. 81 on Dec 3, 2021); b – geophone arranged atop of soil–cement pile (large-scale blast no. 81 on Dec 3, 2021)

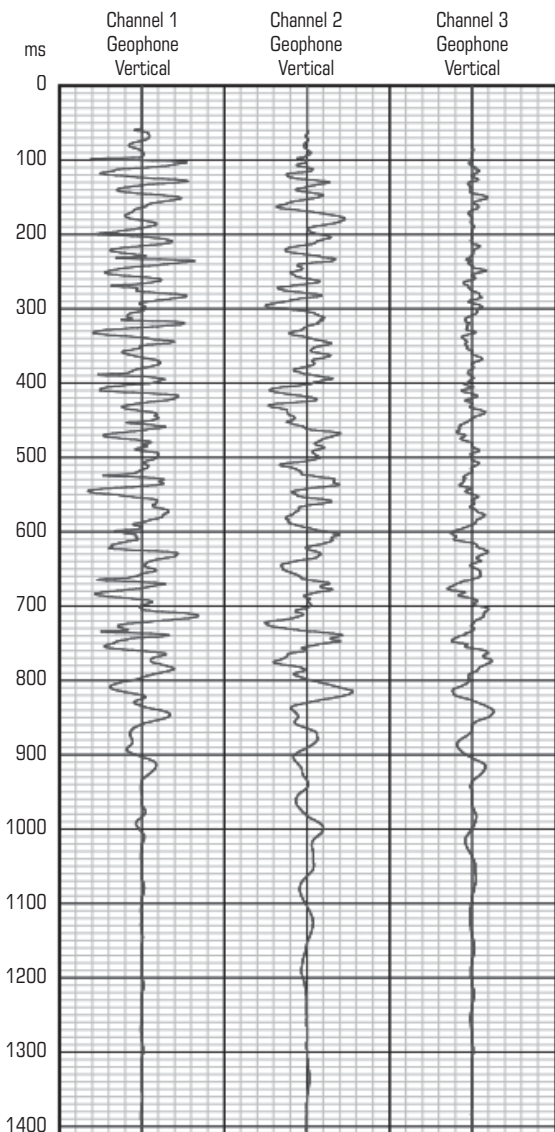


Fig. 3. Representative seismogram from geophone on soil–cement pile top during blast no. 81: $u_2(R) = 5.71 \text{ mm/s}$; $R = 26 \text{ m}$

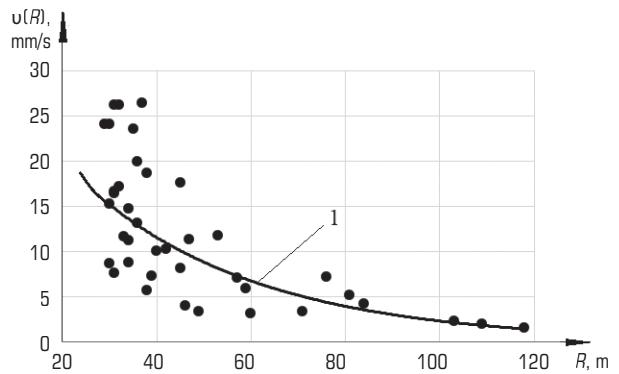


Fig. 4. Function $u(R)$ versus distance R at caisson bottom: • – experiment; 1 – theoretical curve from (3)

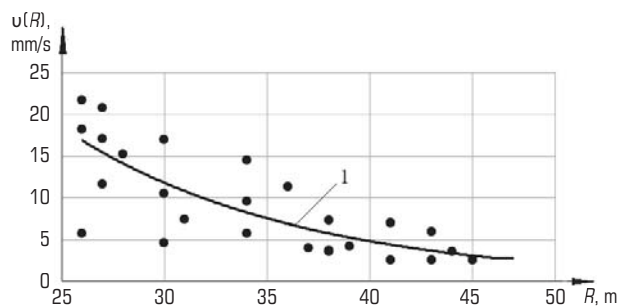


Fig. 5. Function $u(R)$ versus distance R at soil–cement pile top: • – experiment; 1 – theoretical curve from (4)

of the caisson and at the tops of the soil–cement piles (see fig. 1). The placement of geophones at the guarded objects is illustrated in Fig. 2.

The analysis of seismograms (a representative seismogram is given in Fig. 3) allowed correlation of PPV and distances for the caisson (Fig. 4) and soil–cement piles (Fig. 5). In Figs. 4 and 5, the points stand for the experimental results, and the curves depict theoretical relations (5) and (6), respectively.

It is worthy of mentioning that at the distances of 25–40 m (see fig. 4) and 25–30 m (see fig. 5), the scatter in the values of PPV caused by blasting-induced seismic waves is rather large, from 5 to 25 mm/s. Probably, this is connected with reflection of BSW from the retention wall, caisson wall and the soil–cement piles, and with the interference of BSW in sequential blasting. On the whole, the analysis of plots (5) and (6) proves the reliability of formulas (1)–(6). PPV due to BSW is 2.0–27.0 mm/s at the farther wall of the caisson and is 2.0–22.0 mm/s at the nearest wall of the soil–cement piles. These values are much lower than the allowable PPV of 100–500 mm/s. Thus, during blasting and currently, the caisson integrity is preserved, and water inflow from the gulf is kept down.

Conclusions

During construction of a dry dock, it became necessary to level the gneissic granite rock mass soil by 7 m. The blasting site adjoined a reinforced concrete caisson and a cofferdam reinforced with soil–cement piles at a spacing of 8.5–20.0 m. For achieving the required levelling elevation of 16.2 m, fragmentation quality and seismic safety, the parameters associated with the drilling-and-blasting patterns were calculated. The necessary formulas are constructed, and PPV caused by

the blasting-induced seismic waves in the caisson and cofferdam were calculated. The experimental measurement of ground vibrations used seismic recorder Vibracord DX. All in all, 20 large-scale blasts were performed, and the blasted rock volume totaled 9 Km³.

The comparison of the actual and theoretical PPV values in the caisson and soil–cement piles of the cofferdam confirms reliability of the formulas. PPV caused by blasting-induced seismic waves at the farther wall of the caisson and at the closest wall of the soil–cement piles are 2.0–27.0 mm/s and 2.0–22.0 mm/s, respectively, which is much lower than the allowable PPV values of 100–500 mm/s for the hydraulic engineering structures. It has been determined during blasting that the caisson preserves its integrity and no increase in water inflow from the gulf is observed.

References

- Kutuzov B. N. Methods of conducting blasting operations. Part 2. Blasting in mining and industry. Moscow : Gornaya kniga, 2008. 512 p.
- Kutuzov B. N., Tyupin V. N. Drilling and blasting design method to ensure preset fragmentation of rocks in open pit mining. *Gorniy Zhurnal*. 2017. No. 8. pp. 66–69. DOI: 10.17580/gzh.2017.08.12
- Federal Code for Safety in Industry: Safety Regulations for Blasting. Moscow : Publishing House of ZAONTTS PB, 2000. 330 p.
- Belin V. A. Methods of conducting blasting operations. Special blasting operations. Moscow : MGGU, 2007. 563 p.
- Menshikov P. V., Taranjin S. S., Flyagin A. S. Research of seismic influence on buildings and structures of Satka town while exploding explosive works on the Karagayskiy career in constrained conditions. *GIAB*. 2020. No.3-1. pp. 383–398.
- Ekvist B. V. Seismic impact of blasting with nonuniform blasthole pattern design. *Vzrinnoye delo*. 2020. No. 127–84. pp. 135–146.
- Belin V. A., Gorbonos M. G., Astakhov E. O. Influence of primers on blasting efficiency and safety. *Gorniy Zhurnal*. 2017. No. 7. pp. 63–67. DOI: 10.17580/gzh.2017.07.12
- Maslov I. N., Sivenkov V. I., Ilyakhin S. V. et al. Commercial Emulsion Explosives and Initiation Systems in Blasting. Moscow : VNIIGeosystem, 2018. 416 p.
- Shevkun E. B., Leshchinsky A.V., Lysak Yu. A. et al. Long-period delay loosening blasting in open pit mines. *GIAB*. 2020. No. 10. pp. 29–41.
- Adushkin V. V., Anisimov V. N. Geodynamic and geoecological safety and its provision in the Kursk Magnetic Anomaly. *VII International Conference Proceedings (Honor the Memory of Prof. Petin A.N.)—Nature Management and Ecology in European Russia and in Adjacent Areas*. Belgorod : Politerra, 2017. pp. 13–20.
- Sovmen V. K., Kutuzov B. N., Maryasov A. L. et al. Seismic Safety in Blasting. Moscow : Gornaya kniga, 2002. 228 p.
- Korshunov G. I., Bulbasheva I. A., Afanasyev P. I. Blasting-induced seismic impact on power transmission lines. *Occupational safety in industry*. 2019. No. 4. pp. 39–43.
- Zykov V. S., Ivanov V. V., Sobolev V. V. Impact of large-scale blasting on stability of excavations in open and underground mining of coal. *Occupational Safety in Industry*. 2018. No. 11. pp.19–23.
- Tyupin V. N. Geomechanical behavior of jointed rock mass in the large-scale blast impact zone. *Eurasian Mining*. 2020. No. 2. pp. 11–14. DOI: 10.17580/em.2020.02.03.
- Tyupin V. N. Prediction of the ground vibration rate during large-scale explosions in the underground conditions. *Occupational safety in industry*. 2021. No. 6. pp. 41–45. DOI: 10.24000/0409-2961-2021-6-41-45
- Tyupin V. N. Seismic effects induced by large-scale blasts in isotropic and structurally complex pit wall rock masses. *GIAB*. 2021. No. 12. pp. 47–51.
- Agrawal H., Mishra A. K. Modified scaled distance regression analysis approach for prediction of blast-induced ground vibration in multi-hole blasting. *Journal of Rock Mechanics and Geotechnical Engineering*. 2019. Vol. 11, No. 1. pp. 202–207.
- Drover C., Villaescusa E. A comparison of seismic response to conventional and face distress blasting during deep tunnel development. *Journal of Rock Mechanics and Geotechnical Engineering*. 2019. Vol. 11, No. 1. pp. 965–978.
- Fulawka K., Stoletsky L., Proc I. J. et al. Time-frequency characteristic of seismic waves observed in the Lower Silesian copper basin. *19th International Multidisciplinary Scientific GeoConference SGEM 2019*. 2019. Vol. 19. pp. 693–700.
- Onika S. G., Naryzhnova E. J. Seismically safe parameters of explosions in a quarry of natural stone. *Innovative Development of Resource-Saving Technologies of Mineral Mining and Processing : International Scientific and Technical Internet Conference : Book of Abstracts*. Petroşani : Universitas Publishing, 2018. pp. 64–66.
- Gui Y. L., Zhao Z. Y., Jayasinghe L. B. et al. Blast wave induced spatial variation of ground vibration considering field geological conditions. *International Journal of Rock Mechanics and Mining Sciences*. 2018. Vol. 101. pp. 63–68.
- Gospodarikov A. P., Zatsepin M. A. Mathematical modeling of boundary problems in geomechanics. *Gorniy Zhurnal*. 2019. No. 12. pp. 16–20. DOI: 10.17580/gzh.2019.12.03
- Lapin S. E. Forecast of the dynamics of the rock massif state in the processes of coal deposit underground mining. *Occupational safety in industry*. 2019. No. 11. pp. 60–66.
- Sonova M. A., Trofimov A.V., Rummyantsev A. E. et al. Application of numerical and block geomechanical modeling to determine the parameters of fastening chamber workings of large cross-section. *Gornaya promyshlennost*. 2021. No. 2. pp.127–131.
- Kabelko S. G., Ovsyannikov A. N., Konovalov A.V. et al. Predicting the content of useful components in blasted rock mass for real-time planning. *Gorniy Zhurnal*. 2021. No. 6. pp.17–20. 